

Effect of the Center Frequency of Chaotic Signals on the EMI Suppression in DC-DC Converters with Chaotic Modulation

Yuhong Song¹, Zhong Li², Junying Niu¹, Wallace K.S. Tang³ and Wolfgang A. Halang²

¹ School of Electronic and Information Engineering, Shunde Polytechnic, P. R. China

² Faculty of Mathematics and Computer Science, Fernuniversity in Hagen, Germany

³ City University of Hong Kong, Kowloon, Hong Kong

Abstract—Chaotic signals have the characteristics of fluctuant and continuous spectrum waveform due to pseudo-randomness of chaos. The largest peak on the spectrum is defined as the central frequency in this paper. As one kind of spread-spectrum modulation, chaotic duty modulation is adopted to suppress electromagnetic interference (EMI) in switching converters. This paper is concerned with the effect of the center frequency on chaotic modulation for EMI reduction. Simulations and experimental verification are conducted on a DC-DC Buck converter.

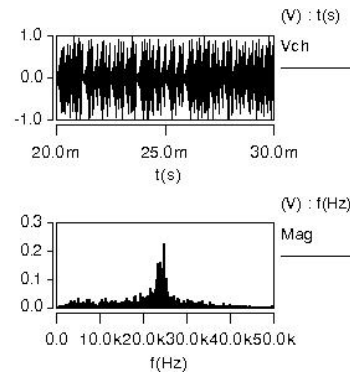


Figure 1: The chaotic signal of Chua’s circuit (upper) and its FFT (lower)

1. Introduction

Due to the pseudo-randomness and continuous spectrum of chaos, chaos control has been widely applied in the security communication, the EMI reduction in power electronics and so on [1, 2, 3]. However, the spectrum waveform of chaos is fluctuant with some peaks and the energies concentrate upon a limited range of frequency[4]. It is reported in [5] that the spectrum range of the chaotic signal is required to match the actual bandwidth of the communication channel in the security communication. In [6] a chaotic frequency modulation has been implemented to reduce EMI by connecting external chua’s chaotic signal to the PWM module of a DC-DC Boost converter, and proposed that the chaotic oscillating frequency should approach the switching one of the converter.

With the overview on related literature, the optimization of chaotic signal should be considered in suppressing EMI with chaotic modulation. This paper defines the frequency of the largest spectrum peak as the center frequency denoted by f_o , which reflects the signal evolving speed and spectral range. The evolving waveform and spectrum of a chaotic signal are demonstrated in Fig.1. The largest spectrum peak locates at the center frequency f_o (for this example, $f_o=24$ KHz). Additionally, the spectrum mainly distribute within the range of $0 \sim 2f_o$.

2. Chaotic Modulation

2.1. Chaotic Duty Modulation

As shown in Fig.2, the circuit is demonstrated for the chaotic duty modulation in a DC-DC Buck converter by injecting the chaotic signal to the PWM module.

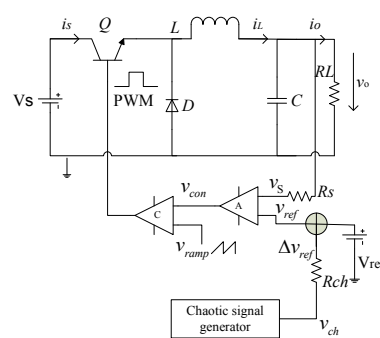


Figure 2: The schematic diagram of chaotic duty modulation

The variable v_{ch} is the external chaotic signal and is linearly processed to be Δv_{ref} through the resistor R_{ch} , denote the linear coefficient by k_1 , there

$$\Delta v_{ref} = k_1 v_{ch}. \quad (1)$$

The variable v_{con} is the control voltage. It is the issue of amplifying the error between v_S and v_{ref} . Assuming that the amplifier gain is constant and denoted by A_1 , v_{con} is described by

$$v_{con} = A_1(v_S - v_{ref}) = A_1(\gamma_1 - V_{ref}) - A_1k_1v_{ch} \quad (2)$$

which exists two parts. One part of the equation is $A_1(\gamma_1 - V_{ref})$, which is constant and denoted by γ_2 . The other one is $A_1k_1v_{ch}$, where A_1k_1 is constant and denoted by γ_3 . Therefore, v_{con} is simplified as

$$v_{con} = \gamma_2 + \gamma_3v_{ch}. \quad (3)$$

Because v_{con} is the result of processing v_{ch} by linearization and translation, v_{con} is also chaotic and the duty of chaotic modulation pulse is consequently chaotic, as shown in Fig.3.

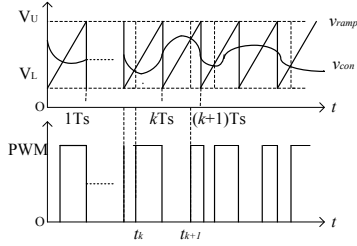


Figure 3: Waveforms of v_{ramp} , v_{con} and chaotic modulation pulse

2.2. Spectrum Analysis

Define the ramp as

$$v_{ramp} = V_L + (V_U - V_L)\left(\frac{t}{T_s} \bmod 1\right) \quad (4)$$

where V_L and V_U are the minimum and maximum values respectively, and T_s is the cycle of the ramp. In Fig.3, the high level starting time t_k of the k th pulse is decided by the crosspoint of v_{con} and v_{ramp} :

$$\begin{aligned} t_k &= (k-1)T_s + \frac{v_{con} - V_L}{V_U - V_L} T_s \\ &= (k-1)T_s + \frac{\gamma_3v_{ch} + \gamma_2 - V_L}{V_U - V_L} T_s. \end{aligned} \quad (5)$$

Denote v_{ch} at the crosspoint by $v_{ch}(k)$ in the k th cycle. In terms of Fourier transformation[7], the spectrum for the k th pulse is expressed as

$$F_k(\omega) = \int_0^{kT_s - t_k} A e^{-j\omega t} dt = \frac{jA}{\omega} [e^{-j\omega(kT_s - t_k)} - 1], \quad (6)$$

further, Eq. (6) can be rewritten as

$$F_k(\omega) = \frac{jA}{\omega} \left[e^{-j\omega \left(T_s - \left(\frac{\gamma_3v_{ch}(k) + \gamma_2 - V_L}{V_U - V_L} T_s \right) \right)} - 1 \right]. \quad (7)$$

Assume $\frac{\gamma_3v_{ch} + \gamma_2 - V_L}{V_U - V_L} = \mu v_{ch} + b_1$, then $\mu = \frac{\gamma_3}{V_U - V_L} > 0$, and $b_1 = \frac{\gamma_2 - V_L}{V_U - V_L} > 0$, So Eq. (7) can be expressed as

$$F_k(\omega) = \frac{jA}{\omega} \left[e^{-j\omega T_s(1 - \mu v_{ch}(k) - b_1)} - 1 \right]. \quad (8)$$

Hence, the spectrum of chaotic modulation pulse denoted by $F(\omega)$ is

$$F(\omega) = \sum_{k=1}^{+\infty} \frac{jA}{\omega} \left[e^{-j\omega T_s(1 - \mu v_{ch}(k) - b_1)} - 1 \right]. \quad (9)$$

From Eq. (9), the $F(\omega)$ is continuous function because of the chaotic PWM pulse. EMI peaks of the converter are commonly known at the fundamental and the harmonics of the switching frequency, so $F(\omega)$ have the extremal points. Denote $n\omega_1$ as angular frequency of the n th harmonic (n is a integer, it represents the fundamental when $n = 1$, otherwise it represents the harmonics). According to Eq. (9), the spectra of the fundamental and the harmonics can be expressed as

$$\begin{aligned} F(\omega_n) &= \sum_{k=1}^{+\infty} \frac{jA}{\omega_n} \left[e^{-j2n\pi(1 - \mu v_{ch}(k) - b_1)} - 1 \right] \\ &= \sum_{k=1}^{+\infty} \frac{jA}{\omega_n} \left[e^{-j2n\pi} e^{j2n\pi\mu v_{ch}(k)} e^{j2nb_1\pi} - 1 \right] \end{aligned} \quad (10)$$

where $e^{-j2n\pi}$ and $e^{j2nb_1\pi}$ are constant, $e^{j2n\pi\mu v_{ch}(k)}$ is variable, and $F(\omega_n)$ varies along with $v_{ch}(k)$. Because $F(\omega_n)$ is the extremal point, there exists extremal values at the fundamental and the harmonics for $e^{j2n\pi\mu v_{ch}(k)}$. In terms of the extremal conditions, one can get $\frac{d(e^{j2n\pi\mu v_{ch}(k)})}{d\omega} = 0$, and $\frac{d^2(e^{j2n\pi\mu v_{ch}(k)})}{d\omega^2} < 0$. Further,

$$\frac{d(e^{j2n\pi\mu v_{ch}(k)})}{d\omega} = j2n\pi\mu e^{j2n\pi\mu v_{ch}(k)} \frac{dv_{ch}(k)}{d\omega}, \quad (11)$$

$$\begin{aligned} \frac{d^2(e^{j2n\pi\mu v_{ch}(k)})}{d\omega^2} &= -(2n\pi\mu)^2 e^{j2n\pi\mu v_{ch}(k)} \left(\frac{dv_{ch}(k)}{d\omega} \right)^2 \\ &+ j2n\pi\mu e^{j2n\pi\mu v_{ch}(k)} \frac{d^2v_{ch}(k)}{d\omega^2}. \end{aligned} \quad (12)$$

When $\frac{dv_{ch}(k)}{d\omega} = 0$, Eq. (11)=0. When $\frac{dv_{ch}(k)}{d\omega} = 0$ and $\frac{d^2v_{ch}(k)}{d\omega^2} < 0$, Eq. (12)<0. Therefore, when v_{ch} spectrum obtains the extremal values at the fundamental and the harmonics of the switching frequency, the modulation pulse spectrum reaches the extremal value. Hence, at the fundamental and the harmonics, v_{ch} spectrum maximizes, $F(\omega_n)$ spectrum also does.

The frequency of the chaotic signal spectrum peak has been defined by center frequency, which is denoted by f_o . Hence, the fundamental and the harmonics of

modulation pulse maximize when f_o equals the switching frequency f_s , as shown in Fig. 4(a). In order to smooth the spectrum peaks of the modulation pulse to suppress EMI, f_o should be deviated from the fundamental and the harmonics of the switching frequency, for example, $f_o = (0.5 + n)f_s$, $n = 0, 1, 2, \dots$. Fig. 4(b) is for $f_o = 0.5f_s$.

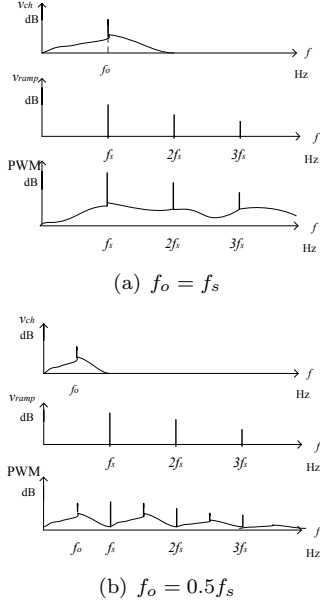


Figure 4: Illustration for spectra of v_{ch} (upper), v_{ramp} (middle) and switching pulse (lower)

3. Chaotic Signal Generator and Center Frequency

Chaotic signals are usually generated by Chua's circuit due to its maturity and simplicity. Chua's circuit consists of one sine oscillator (L_1, C_1, C_2 and R) and one voltage-controlled nonlinear resistor N_r [8], as shown in Fig. 5 including Chua's circuit and $i-v$ characteristic of N_r . N_r can be depicted by one piecewise linear function, m_0 and m_1 are the slopes of external segment and internal one, respectively.

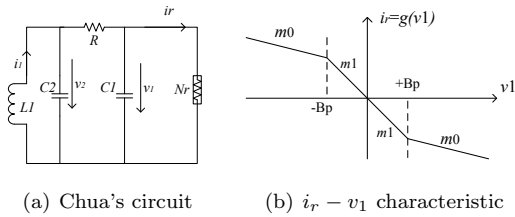


Figure 5: Chua's circuit and N_r characteristic

When Chua's circuit operates in sine period, the oscillation fixes on the center frequency and signal energy focuses on the center frequency and its harmonics.

Table 1: Combinations of parameters and the relative center frequency

| parameters | f_o (kHz) |
|---|-------------|
| $C_1 = 44\text{nF}, C_2 = 396\text{nF}, L_1 = 88\text{mH}$ | 0.7 |
| $C_1 = 22\text{nF}, C_2 = 198\text{nF}, L_1 = 44\text{mH}$ | 1.4 |
| $C_1 = 11\text{nF}, C_2 = 99\text{nF}, L_1 = 22\text{mH}$ | 2.8 |
| $C_1 = 5.5\text{nF}, C_2 = 49.5\text{nF}, L_1 = 11\text{mH}$ | 5.6 |
| $C_1 = 2.7\text{nF}, C_2 = 25\text{nF}, L_1 = 5.5\text{mH}$ | 11.2 |
| $C_1 = 2.45\text{nF}, C_2 = 22.7\text{nF}, L_1 = 5\text{mH}$ | 12.5 |
| $C_1 = 1.70\text{nF}, C_2 = 15.8\text{nF}, L_1 = 3.5\text{mH}$ | 17 |
| $C_1 = 1.45\text{nF}, C_2 = 13.5\text{nF}, L_1 = 3\text{mH}$ | 20.5 |
| $C_1 = 1.20\text{nF}, C_2 = 11.2\text{nF}, L_1 = 2.5\text{mH}$ | 24 |
| $C_1 = 0.95\text{nF}, C_2 = 9.0\text{nF}, L_1 = 2\text{mH}$ | 29 |
| $C_1 = 0.80\text{nF}, C_2 = 7.65\text{nF}, L_1 = 1.7\text{mH}$ | 34.57 |
| $C_1 = 0.76\text{nF}, C_2 = 7.20\text{nF}, L_1 = 1.65\text{mH}$ | 36 |

Once the circuit runs into chaos, the signal energy scatters over an expanded frequency range, which roughly centered by the center frequency. In terms of the oscillation conditions, the center frequency of Chua's circuit can be estimated by[9]

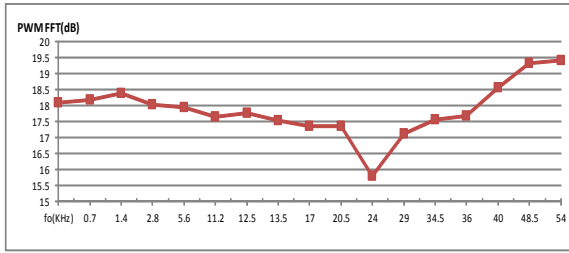
$$f_o = \frac{1}{2\pi\sqrt{L_1 C_2}} \sqrt{1 + \frac{L_1 m_i}{RC_1}}, \text{ and } i = 0, 1. \quad (13)$$

From Eq.(13), different center frequency can be obtained by adjusting the parameters of C_1, C_2 and L_1 [10]. Table 1 lists a set of parameter combinations and the respective center frequency.

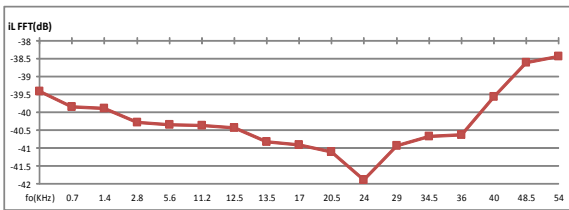
4. Simulations and Experiments

Based on Fig.2, the external chaotic signal v_{ch} is drew from the voltage v_2 of Chua's circuit and the switching frequency f_s is configured as 48 kHz. Simulations are conducted to compare EMI reduction effects with different center frequencies of chaotic signals. The parameters of Chua's circuit are setup according to Table 1. It can be observed in Fig.6 that FFT fundamental amplitudes vary along with the center frequency and the valley appears when $f_o \approx 0.5f_s$, that means the optimal EMI suppression.

The scheme in Fig.2 is realized with hardware, assuming $RL = 1 \Omega, L = 1 \text{ mH}, C = 470 \text{ uF}, V_L = 0 \text{ V}, V_U = 3 \text{ V}, V_s = 25 \text{ V}, V_{\text{ref}} = 2.4 \text{ V}, R_{ch} = 10 \text{ k}\Omega$, and the switching frequency $f_s = 25 \text{ kHz}$. Chaotic signals with $f_o = 24 \text{ kHz}$ and $f_o = 12.5 \text{ kHz}$ are respectively produced by adjusting the parameters of C_1, C_2 and L_1 in Chua's circuit according to Table 1. PWM waveforms and their spectra are shown in Fig.7. It can be observed that the amplitudes of the fundamental and harmonics are more reduced when $f_o = 12.5 \text{ kHz}$ than when $f_o = 24 \text{ kHz}$.

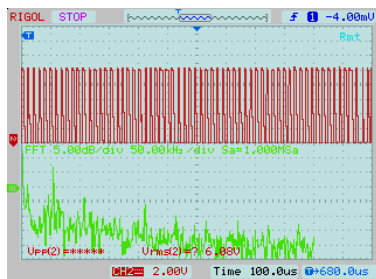


(a) Fundamental amplitudes of PWM FFT

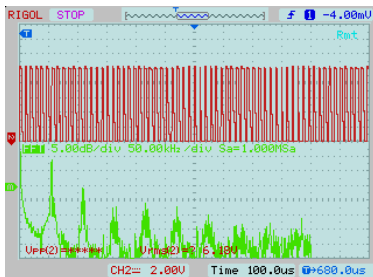


(b) Fundamental amplitudes of i_L FFT

Figure 6: The center frequency vs the amplitude of the fundamental



(a) $f_o = 12.5\text{kHz}$



(b) $f_o = 24\text{kHz}$

Figure 7: The experimental waveforms for switching pulse

5. Conclusions

Chaotic signals characterize the center frequencies over their spectra, and it is proved that the center frequency has an effect on the EMI suppression in switching converters with chaotic modulation in this paper. Simulations and experiments have verified that it is optimal for reducing EMI with chaotic duty modulation when the center frequency of chaotic signal is close

to one half of the switching frequency.

Acknowledgments

This work was supported by AvH-Institutspartnerschaft under grant number 2.4-IP-DEU/1009882.

References

- [1] M. Balestra, M. Lazzarini, G. Setti, and R. Rovati. Experimental performance evaluation of a low-EMI chaos-based current-programmed DC/DC boost converter. In *Circuits and Systems, 2005. ISCAS 2005. IEEE International Symposium on*, pages 1489–1492. IEEE, 2005.
- [2] A. Amini and J. Nazarzadeh. Improvement behavior and chaos control of buck converter in current mode controlled. In *IEEE Int. Conference on Industrial Technology*, pages 1–6. IEEE, 2008.
- [3] H. Li, Z. Li, B. Zhang, W. K. Tang, and W. Halang. Suppressing electromagnetic interference in direct current converters. *Circuits and Systems Magazine, IEEE*, 9(4):10–28, 2009.
- [4] L. Ruan and K. Chen. Chua’s circuit chaotic signal spectrum distribution characteristics and its application in the circuit design. *Journal of circuits and systems*, 3(1):8–13, 1998.
- [5] G. Jiang and Y. Cheng. Study on Chua’s nonlinear chaotic circuit and its frequency characteristic. *Journal of EEE*, 24:5–7, 2002.
- [6] H. Li, Z. Li, B. Zhang, F. Wang, N. Tan, and W. Halang. Design of analogue chaotic PWM for EMI suppression. *Electromagnetic Compatibility, IEEE Transactions on*, 52(4):1001–1007, 2010.
- [7] R. Bracewell. *The fourier transform and its applications 3rd ed.* Boston, McGraw Hill, 2000.
- [8] L. Jackson, A. Lindgren, Y. Kim, *et al.* A chaotic attractor from Chua’s circuit. *IEEE Transactions on Circuits and Systems*, 31(12), 1984.
- [9] A. S. Elwakil and M. P. Kennedy. Improved implementation of Chua’s chaotic oscillator using current feedback op amp. *Circuits and Systems I: Fundamental Theory and Applications, IEEE Transactions on*, 47(1):76–79, 2000.
- [10] M. P. Kennedy. Three steps to chaos. II. a Chua’s circuit primer. *Circuits and Systems I: Fundamental Theory and Applications, IEEE Transactions on*, 40(10):657–674, 1993.